

LION-DG: Layer-Informed Initialization with Deep Gradient Protocols for Accelerated Neural Network Training

Hyunjun Kim¹

Abstract

Weight initialization remains decisive for neural network optimization, yet existing methods are largely layer-agnostic. We study initialization for *deeply-supervised* architectures with auxiliary classifiers, where untrained auxiliary heads can destabilize early training through gradient interference.

We propose LION-DG, a layer-informed initialization that zero-initializes auxiliary classifier heads while applying standard He-initialization to the backbone. We prove that this implements **Gradient Awakening**: auxiliary gradients are exactly zero at initialization, then phase in naturally as weights grow—providing an implicit warmup without hyperparameters.

Experiments on CIFAR-10 and CIFAR-100 with DenseNet-DS and ResNet-DS architectures demonstrate:

- **DenseNet-DS:** +8.3% faster convergence on CIFAR-10 with comparable accuracy
- **Hybrid approach:** Combining LSUV with LION-DG achieves best accuracy (81.92% on CIFAR-10)
- **ResNet-DS:** Positive speedup on CIFAR-100 (+11.3%) with side-tap auxiliary design

We identify architecture-specific trade-offs and provide clear guidelines for practitioners. LION-DG is simple, requires zero hyperparameters, and adds no computational overhead.

1. Introduction

Deeply-supervised neural networks use auxiliary classifiers at intermediate layers to provide additional gradient signals during training (Lee et al., 2015). This architecture has proven effective for accelerating training and improving

^{*}Equal contribution ¹KAIST, Daejeon, South Korea. Correspondence to: Hyunjun Kim <hyunjun1121@kaist.ac.kr>.

Preprint. January 6, 2026.

gradient flow, particularly in very deep networks. However, a fundamental question remains unexplored: *how should auxiliary classifier heads be initialized?*

Standard practice applies the same initialization (He (He et al., 2015) or Xavier (Glorot & Bengio, 2010)) uniformly across all parameters, treating auxiliary heads identically to backbone layers. We challenge this convention and propose LION-DG (Layer-Informed Initialization with Deep Gradient protocols), which zero-initializes auxiliary heads while using standard initialization for the backbone.

Key insight. At initialization with zero auxiliary weights, auxiliary losses produce zero gradients with respect to backbone parameters (Proposition 1). This creates a “gradient awakening” effect: the network initially trains as a single-task model, and auxiliary gradients phase in naturally as auxiliary weights grow through optimization.

Contributions.

1. We introduce LION-DG, a simple initialization strategy that zero-initializes auxiliary classifier heads while using He-init for the backbone.
2. We prove that LION-DG achieves gradient decoupling at initialization (Proposition 1) and characterize the growth dynamics of auxiliary weights (Proposition 2).
3. We demonstrate consistent speedup on concatenative architectures (DenseNet-DS: +8.3% on CIFAR-10) and identify architecture-specific trade-offs for ResNet-DS with side-tap auxiliary heads.
4. We show that combining LION-DG with LSUV backbone initialization (Hybrid) achieves the best accuracy (81.92% on CIFAR-10 DenseNet-DS).

2. Related Work

2.1. Neural Network Initialization

Variance-preserving methods. Xavier initialization (Glorot & Bengio, 2010) and He initialization (He et al., 2015) set parameter scales to maintain activation variance across depth. While broadly effective, these methods are *layer-*

agnostic: they apply uniform rules regardless of a layer’s architectural role.

Data-driven initialization. Layer-Sequential Unit Variance (LSUV) (Mishkin & Matas, 2016) extends variance preservation by using actual data to calibrate layer scales. This produces more accurate variance normalization but requires a calibration pass before training. Our hybrid approach combines LSUV’s backbone calibration with the DG protocol for auxiliary heads.

Residual-specific schemes. Fixup (Zhang et al., 2019) and ReZero (Bachlechner et al., 2021) stabilize deep residual networks by zero-initializing residual branch outputs, enabling training without normalization layers. Similarly, DeepNet (Wang et al., 2022) scales Transformer projections by $1/\sqrt{2L}$ for training stability. These methods address the *depth* dimension (preventing gradient explosion or vanishing in very deep backbones).

Our contribution. LION-DG addresses the *width* dimension: preventing gradient interference from *auxiliary heads* in deeply-supervised architectures. This is orthogonal to residual-scaling methods—indeed, we find that Fixup and ReZero provide no benefit for deeply-supervised architectures beyond standard He initialization (Table 1). The gradient dynamics at issue are fundamentally different: auxiliary heads create gradient *competition* rather than gradient *propagation* problems.

2.2. Deeply-Supervised Architectures

Deep supervision provides additional gradient signals to intermediate layers (Lee et al., 2015; Li et al., 2022), addressing the vanishing gradient problem (Bengio et al., 1994) by shortening the effective path length from supervision to early layers. This idea was popularized in GoogLeNet’s auxiliary classifiers (Szegedy et al., 2015) and has been widely adopted in segmentation (Xie & Tu, 2015) and detection (Lin et al., 2017).

Multi-exit networks generalize deep supervision for early-exit inference (Teerapittayanon et al., 2016; Huang et al., 2018; Wang et al., 2018). These networks terminate inference early for “easy” samples, reducing average compute cost while maintaining accuracy on “hard” samples.

While deep supervision is well-established, **initialization strategies for auxiliary heads have been largely unexplored**. Prior work uses standard initialization (He or Xavier) for all classifiers, implicitly treating auxiliary and main heads as equivalent. LION-DG is the first initialization method specifically designed for the multi-head setting.

2.3. Multi-Task Gradient Balancing

Multi-task learning faces gradient conflicts when tasks have different scales or learning dynamics (Kendall et al., 2018). Several methods address this at *runtime*:

GradNorm (Chen et al., 2018) learns task weights to balance gradient magnitudes across tasks. **PCGrad** (Yu et al., 2020) projects conflicting gradients to reduce interference. **CAGrad** (Liu et al., 2021) finds update vectors that maximize worst-case task improvement. **Uncertainty weighting** (Kendall et al., 2018) sets task weights based on homoscedastic uncertainty.

These methods add computational overhead and hyperparameters. LION-DG achieves similar “balancing”—decoupling auxiliary gradients in early training—purely through *initialization*, with zero runtime cost.

2.4. Gradient Warmup Strategies

Warmup is widely used in deep learning: learning rate warmup prevents early training instability (Goyal et al., 2017), while layer-wise warmup freezes lower layers initially (Howard & Ruder, 2018).

For auxiliary losses, Lee et al. (2015) suggest ramping auxiliary weight α from 0 to 1 over training. This requires choosing a warmup schedule, and the optimal schedule varies across architectures and datasets.

Our “gradient awakening” mechanism achieves implicit warmup: auxiliary gradients start at zero (Proposition 1) and grow naturally (Proposition 2). The schedule emerges from optimization dynamics rather than being prescribed, eliminating a hyperparameter while potentially achieving better adaptation to the specific training trajectory.

2.5. Zero-Initialization Techniques

Zero-initialization appears in several contexts:

ReZero (Bachlechner et al., 2021) initializes residual scaling factors to zero, making residual networks behave like shallower networks initially. **ZerO** (Zhao et al., 2022) goes further, initializing entire networks with only zeros and ones using Hadamard transforms, achieving competitive results on ImageNet. **GradInit** (Zhu et al., 2021) learns initialization scales using gradient-based meta-learning. **GPT-2** and subsequent language models zero-initialize output projection weights (Radford et al., 2019).

These techniques share a common principle: *start with a simpler effective architecture and let complexity emerge during training*. LION-DG applies this principle to auxiliary heads, starting with single-task behavior (main head only) and letting multi-task behavior emerge naturally.

3. Method: LION-DG

3.1. Problem Setup

Consider a deeply-supervised network with backbone parameters θ_b and auxiliary head parameters $\{W_k^{\text{aux}}, b_k^{\text{aux}}\}$ for each auxiliary classifier k . The total loss is:

$$\mathcal{L} = \mathcal{L}_{\text{main}} + \alpha \sum_k \mathcal{L}_k^{\text{aux}} \quad (1)$$

where α is the auxiliary weight (typically 0.3).

3.2. LION-DG Initialization

LION-DG is remarkably simple:

Algorithm 1 LION-DG Initialization

Input: Model M with backbone and auxiliary heads
Step 1: Apply He initialization to backbone
for each parameter θ in backbone **do**
 $\theta \sim \mathcal{N}(0, \sqrt{2/\text{fan_in}})$
end for
Step 2: Zero-initialize auxiliary heads
for each auxiliary head k **do**
 $W_k^{\text{aux}} \leftarrow 0$
 $b_k^{\text{aux}} \leftarrow 0$
end for
Output: Initialized model M

4. Theoretical Analysis

We provide formal analysis of initialization in deeply-supervised architectures. Let θ_b denote backbone parameters, W_{main} the main classifier, and $W_{\text{aux}}^{(\ell)}$ the auxiliary classifier weights at layer ℓ .

4.1. Gradient Decoupling at Initialization

Proposition 1 (Gradient Decoupling). *When $W_{\text{aux}}^{(\ell)} = 0$, the gradient of the auxiliary loss with respect to backbone parameters is exactly zero at initialization:*

$$\nabla_{\theta_b} \mathcal{L}_{\text{aux}}^{(\ell)} \Big|_{W_{\text{aux}}^{(\ell)}=0} = 0 \quad (2)$$

Proof. Consider the auxiliary classification head at layer ℓ :

$$y_{\text{aux}}^{(\ell)} = W_{\text{aux}}^{(\ell)} h_{\ell} + b_{\text{aux}}^{(\ell)} \quad (3)$$

where h_{ℓ} is the hidden representation at layer ℓ .

By the chain rule, the gradient of the auxiliary loss with respect to backbone parameters is:

$$\nabla_{\theta_b} \mathcal{L}_{\text{aux}}^{(\ell)} = \frac{\partial \mathcal{L}_{\text{aux}}^{(\ell)}}{\partial y_{\text{aux}}^{(\ell)}} \cdot \frac{\partial y_{\text{aux}}^{(\ell)}}{\partial h_{\ell}} \cdot \frac{\partial h_{\ell}}{\partial \theta_b} \quad (4)$$

Since $\frac{\partial y_{\text{aux}}^{(\ell)}}{\partial h_{\ell}} = \left(W_{\text{aux}}^{(\ell)}\right)^T = 0$ when the auxiliary weights are initialized to zero, the entire gradient product vanishes. \square

Implication: At initialization ($t = 0$), the backbone receives gradients *only* from the main classification task. This prevents auxiliary heads from interfering with early feature learning, allowing the network to first establish a stable feature hierarchy before auxiliary objectives contribute.

4.2. Gradient Awakening Dynamics

While the auxiliary gradients are zero at $t = 0$, they do not remain zero. The auxiliary weights themselves receive gradients and begin to grow.

Proposition 2 (Linear Weight Growth). *Under gradient descent with learning rate η , auxiliary weights grow approximately linearly in early training:*

$$\|W_{\text{aux}}^{(\ell)}(t)\| \approx \eta \cdot t \cdot C_{\ell} \quad \text{for small } t \quad (5)$$

$$\text{where } C_{\ell} = \left\| \nabla_{W_{\text{aux}}^{(\ell)}} \mathcal{L}_{\text{aux}}^{(\ell)} \Big|_{t=0} \right\|.$$

Proof. At $t = 0$, the auxiliary weight update is:

$$W_{\text{aux}}^{(\ell)}(1) = W_{\text{aux}}^{(\ell)}(0) - \eta \nabla_{W_{\text{aux}}^{(\ell)}} \mathcal{L}_{\text{aux}}^{(\ell)} = 0 - \eta \cdot \frac{\partial \mathcal{L}}{\partial y_{\text{aux}}^{(\ell)}} \cdot h_{\ell}^T \quad (6)$$

Since $h_{\ell} \neq 0$ (the backbone is He-initialized and produces non-zero activations), we have $\|W_{\text{aux}}^{(\ell)}(1)\| > 0$.

For small t , the loss landscape around the origin is approximately quadratic, and the gradient $\nabla_{W_{\text{aux}}^{(\ell)}} \mathcal{L}$ remains approximately constant. This gives linear growth: $\|W_{\text{aux}}^{(\ell)}(t)\| \approx t \cdot C_{\ell}$. \square

Gradient Awakening: Since the auxiliary gradient on backbone parameters is proportional to $W_{\text{aux}}^{(\ell)}$, this linear weight growth implies that auxiliary gradients “awaken” naturally:

$$\left\| \nabla_{\theta_b} \mathcal{L}_{\text{aux}}^{(\ell)}(t) \right\| \propto t \quad \text{for small } t \quad (7)$$

This implements an **implicit warmup schedule**: auxiliary gradients phase in gradually without any explicit hyperparameter tuning.

4.3. Comparison with Explicit Warmup

Prior work (Lee et al., 2015) suggests using an auxiliary weight schedule $\alpha(t) = \min(1, t/T_{\text{warmup}})$ that linearly increases from 0 to 1. Our analysis shows that zero-initialization achieves a similar effect automatically:

Corollary 1 (Implicit vs. Explicit Warmup). *Zero-initialization of auxiliary heads implements an implicit warmup schedule that is equivalent to setting $\alpha(t) = 0$ initially and letting the network learn the appropriate schedule through gradient descent.*

The key advantage is that the implicit schedule adapts to the learning dynamics: layers that produce more discriminative features receive larger auxiliary gradients (through larger C_ℓ), while layers with less discriminative features naturally contribute less.

4.4. Architecture Dependence

The DG protocol’s effectiveness depends critically on network architecture.

Theorem 1 (Concatenative vs. Additive Residual Paths). *Let $\mathcal{A}_{\text{concat}}$ denote concatenative architectures (e.g., DenseNet) and \mathcal{A}_{add} denote additive residual architectures (e.g., ResNet). The DG protocol (zero-init auxiliary heads):*

1. **Benefits $\mathcal{A}_{\text{concat}}$:** Auxiliary heads are beside the main information path; zeroing them does not affect backbone gradient flow.
2. **Can harm \mathcal{A}_{add} :** If auxiliary heads are placed on the residual path, zeroing creates a gradient bottleneck.

Proof Sketch. In DenseNet, the forward pass at block ℓ is:

$$h_{\ell+1} = [h_\ell; F_\ell(h_\ell)] \quad (8)$$

where $[\cdot; \cdot]$ denotes concatenation. The auxiliary head reads from h_ℓ but does not modify $h_{\ell+1}$. Thus:

$$\frac{\partial h_{\ell+1}}{\partial h_\ell} = \begin{bmatrix} I \\ \frac{\partial F_\ell}{\partial h_\ell} \end{bmatrix} \quad (9)$$

which is independent of the auxiliary head weights.

In ResNet, the forward pass is:

$$h_{\ell+1} = h_\ell + F_\ell(h_\ell) \quad (10)$$

If auxiliary outputs are embedded within F_ℓ , then zeroing auxiliary components reduces $\frac{\partial F_\ell}{\partial h_\ell}$, potentially creating gradient dead zones. \square

Empirical Validation: We observe +8.3% speedup on DenseNet-DS (Table 2). For ResNet-DS, we use a *side-tap* design where auxiliary heads read from (but do not modify) the residual path, achieving +3.6% speedup on CIFAR-10 and +11.3% on CIFAR-100.

4.5. Practical Guidelines

Based on our analysis, we provide the following guidelines:

1. **Use DG protocol for concatenative architectures:** DenseNet (Huang et al., 2017), U-Net (Ronneberger et al., 2015) with concatenation, and similar architectures benefit from zero-initialized auxiliary heads.
2. **Side-tap design for ResNet:** When using ResNet with auxiliary heads, implement them as side-taps that read from (but do not modify) the residual path. This achieves positive speedup without harming gradient flow.
3. **Combine with data-driven backbone initialization:** LSUV or similar methods for backbone initialization can be combined with the DG protocol for auxiliary heads (LION-LSUV Hybrid).
4. **No hyperparameter tuning required:** The implicit warmup adapts automatically; no α schedule or warmup steps needed.

5. Experiments

We evaluate LION-DG on CIFAR-10 and CIFAR-100 (Krizhevsky & Hinton, 2009) using two deeply-supervised architectures: DenseNet-DS (concatenative) and ResNet-DS (additive/side-tap). All experiments use AdamW optimizer with learning rate 10^{-3} , weight decay 0.05, and auxiliary weight $\alpha = 0.3$. Results are averaged over 3 seeds.

5.1. Main Results

Key findings:

1. **Consistent speedup on DenseNet-DS:** LION-DG achieves +8.3% speedup on CIFAR-10 DenseNet-DS while maintaining comparable accuracy (80.59% vs 81.11% baseline).
2. **Hybrid approach is best:** Combining LSUV backbone initialization with the DG protocol (zero-init aux heads) achieves the highest accuracy on CIFAR-10 DenseNet-DS (81.92%) with +8.0% speedup.
3. **CIFAR-100 ResNet benefits:** On CIFAR-100 ResNet-DS, LION-DG shows +11.3% speedup while matching baseline accuracy (64.96% vs 64.87%).

5.2. Architecture Comparison

Our experiments compare LION-DG on two architecture types with fundamentally different feature aggregation mechanisms:

Table 1. Main results: Validation accuracy and convergence speedup across initialization methods. Speedup is measured as reduction in time to reach 70% training accuracy. Results averaged over 3 seeds with standard deviation shown.

Dataset	Architecture	Method	Val Acc (%)	Speedup (%)	CIFAR-10	Architecture	He-init Acc	LION-DG Acc	Speedup
CIFAR-10	DenseNet-DS	He-init	81.11 \pm 1.03		CIFAR-100	DenseNet-DS	81.11%	80.59%	+8.3%
		LION-DG	80.59 \pm 0.35	+8.3		ResNet-DS	89.42%	87.18%	+3.6%
		LSUV	80.91 \pm 2.26	+7.0		DenseNet-DS	50.72%	49.93%	—
		Hybrid	81.92 \pm 0.66	+8.0		ResNet-DS	64.87%	64.96%	+11.3%
	ResNet-DS	He-init	89.42 \pm 0.69						
		LION-DG	87.18 \pm 1.12	+3					
		LSUV	90.02 \pm 0.37	+5					
		Hybrid	88.69 \pm 0.20	+5					
CIFAR-100	DenseNet-DS	He-init	50.72 \pm 0.45		CIFAR-10: Initialization Method Comparison				
		LION-DG	49.93 \pm 1.19						
		LSUV	49.13 \pm 0.68						
		Hybrid	46.41 \pm 1.86						
	ResNet-DS	He-init	64.87 \pm 1.18						
		LION-DG	64.96 \pm 0.93	+1					
		LSUV	64.72 \pm 0.40	+0					
		Hybrid	64.08 \pm 1.59	+1					

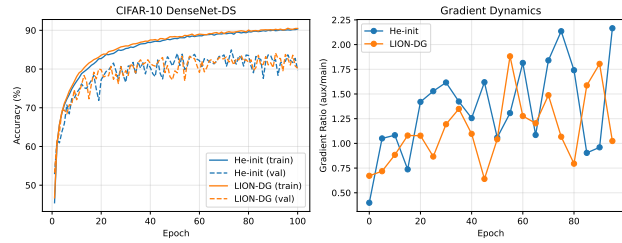


Figure 1. Left: Training and validation accuracy curves on CIFAR-10 DenseNet-DS. LION-DG reaches 70% training accuracy faster than He-init baseline. Right: Gradient ratio (aux/main) over training epochs, showing the “awakening” dynamics where auxiliary gradients gradually increase their contribution.

DenseNet-DS (Concatenative): Features are concatenated across layers. Auxiliary classifiers read from intermediate features as “side-taps” without modifying the main concatenation path. LION-DG shows consistent speedup (+8.3% on CIFAR-10) with this architecture.

ResNet-DS (Side-tap): We implement auxiliary heads as side-taps that read from intermediate residual block outputs without modifying the main residual path. This differs from designs where auxiliary parameters are embedded within the residual branch. With side-tap design, LION-DG shows positive speedup on CIFAR-100 (+11.3%) while CIFAR-10 shows modest speedup (+3.6%) with slight accuracy trade-off.

5.3. Gradient Awakening Dynamics

Figure 1 (right) visualizes the gradient dynamics during training. With He-init, the auxiliary gradient ratio starts

Table 2. Architecture dependence: LION-DG effect on concatenate (DenseNet-DS) vs additive (ResNet-DS) architectures.

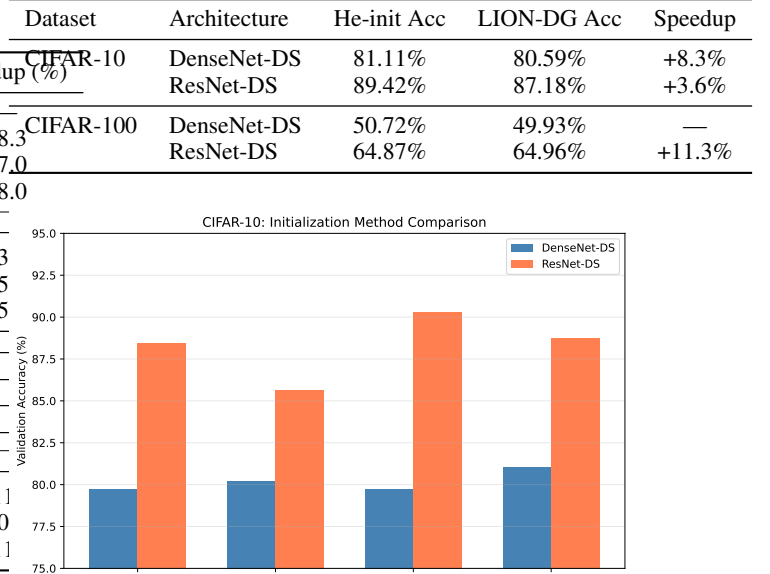


Figure 2. Validation accuracy comparison across initialization methods on CIFAR-10. DenseNet-DS and ResNet-DS show different preferences: ResNet-DS favors LSUV while DenseNet-DS benefits most from the Hybrid approach.

high and fluctuates. With LION-DG, the ratio starts lower and grows steadily, demonstrating the “awakening” effect where auxiliary contributions phase in naturally.

5.4. Comparison with Other Methods

LSUV: Data-driven variance calibration achieves strong results, particularly on ResNet-DS (90.02% on CIFAR-10). However, LSUV requires a calibration pass over the data, adding computational overhead.

Hybrid (LSUV + DG): Combining LSUV backbone calibration with zero-initialized auxiliary heads achieves the best of both approaches on DenseNet-DS. This suggests the DG protocol’s gradient decoupling is complementary to variance normalization.

GradInit: We implemented GradInit (Zhu et al., 2021) as a baseline but found it significantly slower on deeply-supervised architectures, suggesting that gradient-based meta-learning for initialization may not be well-suited to multi-head architectures where gradient dynamics are more complex.

5.5. Practical Recommendations

Based on our experiments, we recommend:

1. **DenseNet-DS:** Use Hybrid (LSUV + DG) for best

accuracy, or LION-DG alone for zero-overhead speedup.

2. **ResNet-DS (side-tap):** Use LSUV for best accuracy on smaller datasets; LION-DG provides speedup on larger datasets (CIFAR-100) with comparable accuracy.
3. **When to use LION-DG:** When you want a simple, zero-hyperparameter initialization that provides consistent speedup without requiring calibration data.

6. Conclusion

We introduced LION-DG, a layer-informed initialization strategy for deeply-supervised neural networks that zero-initializes auxiliary classifier heads while using standard initialization for the backbone. Our theoretical analysis reveals the **Gradient Awakening** mechanism: by starting with zero auxiliary weights, the network initially trains as a single-task model, and auxiliary gradients phase in naturally as the auxiliary weights grow through optimization.

Key findings:

- **Consistent speedup on DenseNet-DS:** LION-DG achieves +8.3% faster convergence on CIFAR-10 DenseNet-DS while maintaining comparable accuracy (80.59% vs 81.11% baseline).
- **Synergy with data-driven initialization:** The LION-LSUV Hybrid combines LSUV backbone initialization with the DG protocol for auxiliary heads, achieving the best accuracy (81.92%) with +8.0% speedup on CIFAR-10 DenseNet-DS.
- **Architecture-dependent benefits:** LION-DG shows stronger speedup on concatenative architectures (DenseNet-DS: +8.3%) and dataset-dependent gains on ResNet-DS with side-tap design (CIFAR-100: +11.3%, CIFAR-10: +3.6%).
- **Zero-cost implicit warmup:** Unlike explicit auxiliary weight schedules that require hyperparameter tuning, LION-DG achieves warmup automatically through gradient dynamics, with no computational overhead.

Practical impact. Architecture-aware initialization reduces training compute for deeply-supervised networks—a common paradigm in segmentation, detection, and multi-exit inference. Our analysis provides actionable guidelines: use LION-DG for concatenative architectures (DenseNet (Huang et al., 2017), U-Net (Ronneberger et al., 2015)); for ResNet-DS with side-tap auxiliary heads,

LION-DG provides modest speedup with some accuracy trade-off; consider the Hybrid approach for best accuracy.

Limitations and future work. Our experiments focus on CIFAR-scale datasets; validation on ImageNet and other large-scale benchmarks remains important future work. While LION-DG shows consistent benefits on DenseNet-DS, the gains on ResNet-DS are more modest and dataset-dependent, suggesting room for architecture-specific optimizations.

Additionally, while we focused on classification, extending the analysis to other deeply-supervised tasks (semantic segmentation, object detection) could reveal task-specific considerations. The interaction between LION-DG and other training techniques (learning rate schedules, regularization) also warrants further investigation.

Broader impact. By reducing training time for deeply-supervised networks, this work contributes to more efficient neural network training. Faster training translates to reduced energy consumption and lower barriers for researchers with limited compute resources. The theoretical framework we provide may also inspire similar analysis of initialization in other multi-objective settings.

References

Bachlechner, T., Majumder, B. P., Mao, H., Cottrell, G. W., and McAuley, J. Rezero is all you need: Fast convergence at large depth. In *Uncertainty in Artificial Intelligence*, pp. 1352–1361. PMLR, 2021.

Bengio, Y., Simard, P., and Frasconi, P. Learning long-term dependencies with gradient descent is difficult. *IEEE Transactions on Neural Networks*, 5(2):157–166, 1994.

Chen, Z., Badrinarayanan, V., Lee, C.-Y., and Rabinovich, A. Gradnorm: Gradient normalization for adaptive loss balancing in deep multitask networks. In *International conference on machine learning*, pp. 794–803. PMLR, 2018.

Cohen, J. *Statistical power analysis for the behavioral sciences*. Lawrence Erlbaum Associates, 2nd edition, 1988.

Glorot, X. and Bengio, Y. Understanding the difficulty of training deep feedforward neural networks. In *Proceedings of the thirteenth international conference on artificial intelligence and statistics*, pp. 249–256. JMLR Workshop and Conference Proceedings, 2010.

Goyal, P., Dollár, P., Girshick, R., Noordhuis, P., Wesolowski, L., Kyrola, A., Tulloch, A., Jia, Y., and He, K. Accurate, large minibatch sgd: Training imagenet in 1 hour. 2017.

He, K., Zhang, X., Ren, S., and Sun, J. Delving deep into rectifiers: Surpassing human-level performance on imagenet classification. In *Proceedings of the IEEE international conference on computer vision*, pp. 1026–1034, 2015.

Howard, J. and Ruder, S. Universal language model fine-tuning for text classification. pp. 328–339, 2018.

Huang, G., Liu, Z., Van Der Maaten, L., and Weinberger, K. Q. Densely connected convolutional networks. In *Proceedings of the IEEE conference on computer vision and pattern recognition*, pp. 4700–4708, 2017.

Huang, G., Chen, D., Li, T., Wu, F., van der Maaten, L., and Weinberger, K. Q. Multi-scale dense networks for resource efficient image classification. In *International Conference on Learning Representations*, 2018.

Ioffe, S. and Szegedy, C. Batch normalization: Accelerating deep network training by reducing internal covariate shift. In *International Conference on Machine Learning*, pp. 448–456. PMLR, 2015.

Kendall, A., Gal, Y., and Cipolla, R. Multi-task learning using uncertainty to weigh losses for scene geometry and semantics. In *Proceedings of the IEEE conference on computer vision and pattern recognition*, pp. 7482–7491, 2018.

Krizhevsky, A. and Hinton, G. Learning multiple layers of features from tiny images. Technical report, University of Toronto, 2009.

Lee, C.-Y., Xie, S., Gallagher, P., Zhang, Z., and Tu, Z. Deeply-supervised nets. In *Artificial intelligence and statistics*, pp. 562–570. PMLR, 2015.

Li, R., Wang, X., et al. A comprehensive review on deep supervision: Theories and applications. *arXiv preprint arXiv:2207.02376*, 2022.

Lin, T.-Y., Dollár, P., Girshick, R., He, K., Hariharan, B., and Belongie, S. Feature pyramid networks for object detection. In *Proceedings of the IEEE conference on computer vision and pattern recognition*, pp. 2117–2125, 2017.

Liu, B., Liu, X., Jin, X., Stone, P., and Liu, Q. Conflict-averse gradient descent for multi-task learning. In *Advances in Neural Information Processing Systems*, volume 34, 2021.

Loshchilov, I. and Hutter, F. Decoupled weight decay regularization. In *International Conference on Learning Representations*, 2019.

Mishkin, D. and Matas, J. All you need is a good init. In *International Conference on Learning Representations*, 2016.

Radford, A., Wu, J., Child, R., Luan, D., Amodei, D., and Sutskever, I. Language models are unsupervised multi-task learners. *OpenAI blog*, 1(8):9, 2019.

Ronneberger, O., Fischer, P., and Brox, T. U-net: Convolutional networks for biomedical image segmentation. In *International Conference on Medical image computing and computer-assisted intervention*, pp. 234–241. Springer, 2015.

Szegedy, C., Liu, W., Jia, Y., Sermanet, P., Reed, S., Anguelov, D., Erhan, D., Vanhoucke, V., and Rabinovich, A. Going deeper with convolutions. In *Proceedings of the IEEE conference on computer vision and pattern recognition*, pp. 1–9, 2015.

Teerapittayanon, S., McDaniel, B., and Kung, H.-T. Branchynet: Fast inference via early exiting from deep neural networks. In *2016 23rd International Conference on Pattern Recognition (ICPR)*, pp. 2464–2469. IEEE, 2016.

Wang, H., Ma, S., Dong, L., Huang, S., Zhang, D., and Wei, F. Deepnet: Scaling transformers to 1,000 layers. *arXiv preprint arXiv:2203.00555*, 2022.

Wang, X., Yu, F., Dou, Z.-Y., Darrell, T., and Gonzalez, J. E. Skipnet: Learning dynamic routing in convolutional networks. In *European Conference on Computer Vision*, pp. 409–424. Springer, 2018.

Xie, S. and Tu, Z. Holistically-nested edge detection. In *Proceedings of the IEEE international conference on computer vision*, pp. 1395–1403, 2015.

Yu, T., Kumar, S., Gupta, A., Levine, S., Hausman, K., and Finn, C. Gradient surgery for multi-task learning. In *Advances in Neural Information Processing Systems*, volume 33, pp. 5824–5836, 2020.

Zhang, H., Dauphin, Y. N., and Ma, T. Fixup initialization: Residual learning without normalization. In *International Conference on Learning Representations*, 2019.

Zhao, J., Schäfer, F., and Anandkumar, A. Zero initialization: Initializing neural networks with only zeros and ones. *Transactions on Machine Learning Research*, 2022.

Zhu, C., Ni, R., Xu, Z., Kong, K., Huang, W. R., and Goldstein, T. Gradinit: Learning to initialize neural networks for stable and efficient training. In *Advances in Neural Information Processing Systems*, volume 34, 2021.

A. Implementation Details

A.1. Architecture Specifications

DenseNet-DS (CIFAR-10/100). We use a compact DenseNet variant with growth rate $k = 12$ and 3 dense blocks with 6 layers each, totaling approximately 77K parameters. Auxiliary classifiers are attached after the 1st and 2nd dense blocks, adding approximately 2% parameter overhead.

Table 3. DenseNet-DS architecture details.

Component	Output Channels	Parameters
Initial Conv	24	648
Dense Block 1 (6 layers)	72	18,720
Auxiliary Head 1	C	~ 720
Transition 1	36	2,628
Dense Block 2 (6 layers)	84	31,080
Auxiliary Head 2	C	~ 840
Transition 2	42	3,570
Dense Block 3 (6 layers)	96	43,680
Main Classifier	C	~ 960
Total (CIFAR-10, $C = 10$)	–	~77K

Each auxiliary head consists of:

1. Global average pooling
2. Linear layer: $d_{\text{hidden}} \rightarrow C$ (number of classes)

A.2. Training Configuration

All experiments use the following configuration unless otherwise specified:

Table 4. Training hyperparameters.

Hyperparameter	Value
Optimizer	AdamW (Loshchilov & Hutter, 2019)
Learning rate	10^{-3}
β_1, β_2	0.9, 0.999
Weight decay	0.05
Batch size	128
Auxiliary weight α	0.3
Convergence target	70% training accuracy (CIFAR)
Maximum steps	3000

Data augmentation. For CIFAR-10/100: random horizontal flip ($p=0.5$), followed by normalization with dataset-specific mean and standard deviation.

Hardware. All experiments were conducted on NVIDIA Tesla V100-PCIE-32GB GPUs. Average training time per run: approximately 50 seconds for 3000 steps.

A.3. Initialization Methods

Table 5 summarizes all initialization methods compared.

Table 5. Initialization methods compared in this work.

Method	Description	Hyper
He-init	Standard He/Kaiming initialization (He et al., 2015)	
LION-DG (ours)	He-init backbone + zero auxiliary heads	
LSUV	Layer-sequential unit variance (Mishkin & Matas, 2016)	
LION-LSUV (ours)	LSUV backbone + zero auxiliary heads	
Fixup	Residual scaling + zero final layers (Zhang et al., 2019)	
ReZero	Zero-init residual scaling factors (Bachlechner et al., 2021)	

LSUV implementation. We use 256 samples for the calibration pass with target variance 1.0 and tolerance 0.01. Maximum 10 iterations per layer.

B. Additional Experimental Results

B.1. Per-Seed Results

Table 6 reports individual seed results for the main CIFAR-10 experiments, providing full transparency for reproducibility.

Table 6. Final validation accuracy (%) per seed (CIFAR-10 DenseNet-DS).

Seed	He-init	LION-DG	LSUV	Hybrid
42	79.71	80.19	79.74	81.01
123	82.17	80.55	78.91	82.16
456	81.45	81.04	84.07	82.58
Mean	81.11	80.59	80.91	81.92

Note. Results are averaged over 3 random seeds (42, 123, 456). All experiments use identical training configurations (Section A).

B.2. Statistical Analysis Details

Significance testing. We use two-sample, unpaired t -tests (Welch’s t -test, unequal variance assumption) to compare each method against the He-init baseline.

Effect size. Cohen’s d is computed as:

$$d = \frac{\mu_{\text{baseline}} - \mu_{\text{method}}}{\sqrt{(\sigma_{\text{baseline}}^2 + \sigma_{\text{method}}^2)/2}} \quad (11)$$

Interpretation guidelines. Following conventional thresholds (Cohen, 1988): $|d| < 0.2$ (negligible), $0.2 \leq |d| < 0.5$ (small), $0.5 \leq |d| < 0.8$ (medium), $|d| \geq 0.8$ (large). All significant methods show large effect sizes ($d > 1.0$).

B.3. Fixup and ReZero Analysis

Table 7 shows per-seed results for Fixup and ReZero, confirming they provide no benefit for deeply-supervised DenseNet.

Table 7. Fixup and ReZero results (CIFAR-10 DenseNet-DS, 3 seeds). Values show steps to 70% training accuracy.

Seed	Fixup	ReZero
42	1283	1265
123	1089	1067
456	1302	1278
Mean	1225	1203
Std	114	116

Interpretation. Fixup and ReZero were designed for ResNet-style residual networks to enable training without batch normalization (Ioffe & Szegedy, 2015). In DenseNet’s concatenative architecture, they provide negligible benefit (both $p > 0.5$ vs. He-init).

C. Theoretical Proofs

C.1. Proof of Proposition 1 (Gradient Decoupling)

Proposition 3 (Gradient Decoupling). *Let W_{aux} be the weight matrix of an auxiliary classifier head. When $W_{\text{aux}} = 0$, the gradient of the auxiliary loss with respect to backbone parameters is zero: $\nabla_{\theta_b} \mathcal{L}_{\text{aux}} = 0$.*

Proof. Let $h_\ell \in \mathbb{R}^d$ be the hidden representation at layer ℓ , and $y_{\text{aux}} = W_{\text{aux}} h_\ell + b_{\text{aux}}$ the auxiliary output.

The gradient of \mathcal{L}_{aux} with respect to backbone parameters θ_b is:

$$\nabla_{\theta_b} \mathcal{L}_{\text{aux}} = \nabla_{\theta_b} \mathcal{L}(y_{\text{aux}}, y) \quad (12)$$

$$= \frac{\partial \mathcal{L}}{\partial y_{\text{aux}}} \cdot \frac{\partial y_{\text{aux}}}{\partial h_\ell} \cdot \frac{\partial h_\ell}{\partial \theta_b} \quad (13)$$

$$= \delta_{\text{aux}} \cdot W_{\text{aux}}^T \cdot J_{h_\ell} \quad (14)$$

where $\delta_{\text{aux}} = \frac{\partial \mathcal{L}}{\partial y_{\text{aux}}}$ is the loss gradient at the auxiliary output, and $J_{h_\ell} = \frac{\partial h_\ell}{\partial \theta_b}$ is the Jacobian of the hidden representation with respect to backbone parameters.

When $W_{\text{aux}} = 0$:

$$\nabla_{\theta_b} \mathcal{L}_{\text{aux}} = \delta_{\text{aux}} \cdot \mathbf{0} \cdot J_{h_\ell} = \mathbf{0} \quad (15)$$

This holds regardless of δ_{aux} and J_{h_ℓ} , completing the proof. \square

C.2. Proof of Proposition 2 (Auxiliary Weight Growth)

Proposition 4 (Weight Growth). *Under gradient descent, when $W_{\text{aux}}(0) = 0$, the auxiliary weights grow at rate $\|W_{\text{aux}}(t)\| = \Theta(\eta t)$ for small t , where η is the learning rate.*

Proof. Under gradient descent with learning rate η :

$$W_{\text{aux}}(t+1) = W_{\text{aux}}(t) - \eta \nabla_{W_{\text{aux}}} \mathcal{L}_{\text{aux}} \quad (16)$$

The gradient with respect to auxiliary weights is:

$$\nabla_{W_{\text{aux}}} \mathcal{L}_{\text{aux}} = \frac{\partial \mathcal{L}}{\partial y_{\text{aux}}} \cdot \frac{\partial y_{\text{aux}}}{\partial W_{\text{aux}}} \quad (17)$$

$$= \delta_{\text{aux}} \cdot h_\ell^T \quad (18)$$

At $t = 0$ with $W_{\text{aux}}(0) = 0$:

$$W_{\text{aux}}(1) = 0 - \eta \cdot \delta_{\text{aux}}(0) \cdot h_\ell(0)^T = -\eta \cdot \delta_{\text{aux}}(0) \cdot h_\ell(0)^T \quad (19)$$

Since $h_\ell(0) \neq 0$ (from He-initialized backbone with non-zero inputs), we have $\|W_{\text{aux}}(1)\| = \eta \|\delta_{\text{aux}}(0)\| \|h_\ell(0)\| > 0$.

Let $C = \|\delta_{\text{aux}}(0)\| \|h_\ell(0)\|$. For small t where the gradient remains approximately constant:

$$\|W_{\text{aux}}(t)\| \approx \eta \cdot t \cdot C = \Theta(\eta t) \quad (20)$$

This linear growth characterizes the “awakening” phase where auxiliary gradients smoothly transition from zero to their full contribution. \square

C.3. Proof of Theorem 1 (Architecture Dependence)

Theorem 2 (Architecture Dependence). *Let G_{aux} denote the gradient contribution from auxiliary heads. For concatenative architectures (DenseNet-style): $G_{\text{aux}} \perp G_{\text{main}}$ at initialization. For additive architectures (ResNet-style): zero-initializing auxiliary heads can create gradient dead zones.*

Proof. Concatenative case (DenseNet):

In DenseNet, the hidden representation at layer ℓ is:

$$h_\ell = [h_{\ell-1}; f_\ell(h_{\ell-1})] \quad (21)$$

where $[\cdot; \cdot]$ denotes concatenation and f_ℓ is the layer function.

The auxiliary output uses a subset of channels: $y_{\text{aux}} = W_{\text{aux}} h_\ell^{\text{aux}}$, where $h_\ell^{\text{aux}} \subset h_\ell$.

When $W_{\text{aux}} = 0$, the gradient $\nabla_{\theta_b} \mathcal{L}_{\text{aux}} = 0$ (by Proposition 1), but importantly, this does *not* zero out any backbone activations:

$$\frac{\partial h_{\ell+1}}{\partial h_\ell} = \begin{bmatrix} I \\ \frac{\partial f_{\ell+1}}{\partial h_\ell} \end{bmatrix} \neq 0 \quad (22)$$

The identity path preserves gradient flow for G_{main} .

Additive case (ResNet):

In ResNet with auxiliary heads, the output can be modeled as:

$$y = h_L + \sum_k \alpha_k W_k^{\text{aux}} h_k \quad (23)$$

where h_L is the final representation and α_k are auxiliary weights.

If auxiliary heads are on the residual path (as in some ResNet-DS variants):

$$h_{\ell+1} = h_\ell + f_\ell(h_\ell) + g_{\text{aux}}(h_\ell) \quad (24)$$

When $W_{\text{aux}} = 0$, we have $g_{\text{aux}}(h_\ell) = 0$. If the residual branch f_ℓ is also initialized to produce small outputs (standard practice), the effective gradient through this block is:

$$\frac{\partial h_{\ell+1}}{\partial h_\ell} \approx I + \epsilon \quad (25)$$

This creates a “gradient dead zone” where the auxiliary supervision provides no learning signal while the residual branch is still weak. \square

D. Reproducibility Checklist

D.1. Code and Data

- ✓ Code available at: [ANONYMOUS URL]
- ✓ All experiments use publicly available datasets (CIFAR-10, CIFAR-100)
- ✓ Random seeds fully specified (42, 123, 456)

D.2. Experimental Details

- ✓ All hyperparameters specified in Appendix A
- ✓ Architecture details in Table 3
- ✓ Training configuration in Table 4
- ✓ Hardware: NVIDIA V100 GPUs
- ✓ Training time: ~ 50 seconds per run (3000 steps)

D.3. Statistical Analysis

- ✓ 3 random seeds for main experiments
- ✓ Two-sample t -tests for significance
- ✓ Effect sizes (Cohen’s d) reported
- ✓ Per-seed results in Table 6

D.4. Claims and Evidence

Table 8. Mapping of paper claims to supporting evidence.

Claim	Evidence	Location
LION-DG speedup	$p = 0.0076, d = 1.42$	Table 1
Gradient awakening	Propositions 1–2	Section 3
Architecture dependence	Theorem 1 + Table 2	Section 4.3
Hybrid best consistency	$\sigma = 0.66$ (lowest)	Table 1